2008

Improving the Ocean Initialization of Coupled Hurricane–Ocean Models Using Feature-Based Data Assimilation

Richard M. Yablonsky
University of Rhode Island

Isaac Ginis
University of Rhode Island, iginis@uri.edu

Citation/Publisher Attribution

Yablonsky, R. M., & Ginis, I. (2008). Improving the Ocean Initialization of Coupled Hurricane–Ocean Models Using Feature-Based Data Assimilation. *Monthly Weather Review, 136*, 2592-2607. doi: 10.1175/2007MWR2166.1
Available at: https://doi.org/10.1175/2007MWR2166.1

Improving the Ocean Initialization of Coupled Hurricane–Ocean Models Using Feature-Based Data Assimilation

Improving the Ocean Initialization of Coupled Hurricane–Ocean Models Using Feature-Based Data Assimilation

RICHARD M. YABLONSKY AND ISAAC GINIS

Graduate School of Oceanography, University of Rhode Island, Narragansett, Rhode Island

(Manuscript received 6 February 2007, in final form 5 October 2007)

ABSTRACT

Coupled hurricane–ocean forecast models require proper initialization of the ocean thermal structure. Here, a new feature-based (F-B) ocean initialization procedure in the GFDL/University of Rhode Island (URI) coupled hurricane prediction system is presented to account for spatial and temporal variability of mesoscale oceanic features in the Gulf of Mexico, including the Loop Current (LC), Loop Current eddies [i.e., warm-core rings (WCRs)], and cold-core rings (CCRs). Using only near-real-time satellite altimetry for the "SHA-assimilated" case, the LC, a single WCR, and a single CCR are assimilated into NAVOCEANO's Global Digitized Environmental Model (GDEM) ocean temperature and salinity climatology along with satellite-derived daily sea surface temperature (SST) data from 15 September 2005 to produce a more realistic three-dimensional temperature field valid on the model initialization date (15 September 2005). For the "fully assimilated" case, both near-real-time altimetry *and* real-time in situ airborne XBT (AXBT) temperature profiles are assimilated into GDEM along with SST to produce the three-dimensional temperature field. Vertical profiles from the resulting SHA-assimilated and fully assimilated temperature fields are compared to 18 real-time AXBT temperature profiles, the ocean climatology (GDEM), and an alternative data-assimilated product [the daily North and Equatorial Atlantic Ocean Prediction System Best Estimate (RSMAS HYCOM), which uses an Optimal Interpolation (OI) based assimilation technique] to determine the relative accuracy of the F-B initialization procedure presented here. Also, the tropical cyclone heat potential (TCHP) from each of these profiles is calculated by integrating the oceanic heat content from the surface to the depth of the 26°C isotherm. Assuming the AXBT profiles are truth, the TCHP rms error for the F-B SHA-assimilated case, the F-B fully assimilated case, the GDEM ocean climatology, and the RSMAS HYCOM product is 12, 10, 45, and 26 kJ cm^{-2}, respectively.

1. Introduction

Hurricanes develop and are maintained by heat energy they receive from the sea surface. The warmer the sea surface temperature (SST) is below the hurricane, the more energy is available to the hurricane (e.g., Emanuel 1986, 1999). Wind-induced mixing of the upper ocean by a hurricane can cool the sea surface via entrainment of cooler water into the oceanic mixed layer (OML) from below (e.g., Shay et al. 1992; Ginis 2002). Therefore, the future intensity of a given hurricane depends not only on the initial temperature of the sea surface below the hurricane but also on the magnitude of the wind-induced sea surface cooling in the region providing heat energy to the hurricane (Bender and Ginis 2000; Shay et al. 2000; Cione and Uhlhorn 2003). The magnitude of the wind-induced cooling depends on the magnitude of the surface wind stress, the depth of the OML, and the temperature gradient at the base of the OML (e.g., Price 1981).

In order for a hurricane prediction model to capture the effect of wind-induced sea surface cooling, it must be coupled to an ocean prediction model. Since an uncoupled hurricane model is restricted by a static SST valid only at the initialization time, the resulting hurricane forecast is necessarily nonphysical except in rare cases where the wind-induced sea surface cooling is negligible (Bender and Ginis 2000). Even if an uncoupled hurricane model forecast is accurate, the danger exists that the forecast is right for the wrong reason. For example, model air–sea fluxes for a given storm case may be tuned to optimize that particular storm's forecast intensity, but if the flux parameterization is not

Corresponding author address: R. Yablonsky, Graduate School of Oceanography, University of Rhode Island, Narragansett, RI 02882.
E-mail: ryablonsky@gso.uri.edu

DOI: 10.1175/2007MWR2166.1

changed, a model forecast for another storm that either goes over a different part of the ocean or goes over the same place at a different time when the SST is similar but the OML depth is different would likely be less accurate. So, even though proper parameterization of air–sea fluxes is extremely important and much work still needs to be done in this area, the tuning of flux parameters should be done in tandem with accurate ocean initialization of a coupled model.

The Geophysical Fluid Dynamics Laboratory (GFDL)/University of Rhode Island (URI) coupled hurricane prediction system (hereafter GFDL model) has been run operationally at the National Oceanic and Atmospheric Administration's (NOAA) National Centers for Environmental Prediction (NCEP) to forecast hurricane track and intensity since 2001 (Bender et al. 2007; Falkovich et al. 2005, hereafter FGL05). From 2001 to 2007, yearly upgrades were made to the atmospheric and/or ocean components of the GFDL model, and one of the major improvements has been the ocean initialization procedure. One major challenge for proper ocean initialization in a coupled hurricane–ocean model is accurate representation of mesoscale oceanic features that do not follow an annual (or even a regular) cycle, such as the penetration of the Loop Current (LC) into the Gulf of Mexico (GoM) and the shedding (and perhaps reattachment) of Loop Current eddies (LCEs; e.g., Oey et al. 2005). For these features, neither a monthly climatology nor a set of historical observations is sufficient, and the potential improvement afforded by near-real-time observations is well documented (e.g., Goni and Trinanes 2003; Goni et al. 2003). In the GFDL model initialization procedure, the climatological LC position and structure are now adjusted and LCEs are now directly inserted using a feature-based (F-B) modeling procedure with real-time in situ and/or remotely sensed observations.

Scientists at NOAA's Hurricane Research Division (HRD) occasionally measure ocean temperature profiles in the prehurricane environment via airborne expendable bathythermograph (AXBT) instruments dropped from aircraft (Cione and Uhlhorn 2003). As the thermistor on the AXBT descends from the sea surface, it provides accurate, high-resolution measurements (every 1.5 m) of the ocean temperature to a depth of ~350–450 m. In section 3, it will be shown how AXBT profiles can be directly assimilated into the ocean model initialization procedure to adjust the position of oceanic features such as the LC or LCEs and to validate model temperature profiles.

The goals of this paper are (i) to describe the most recent version of the GFDL model ocean initialization, including a data assimilation strategy in the Gulf of Mexico, (ii) to evaluate the accuracy of this initialization using in situ data, and (iii) to compare the results to an alternative data-assimilated ocean product, the daily North and Equatorial Atlantic Ocean Prediction System Best Estimate (RSMAS HYCOM, described in section 3b).

2. Ocean initialization in the GFDL/URI coupled hurricane prediction system

The starting point for the ocean initialization in any operational GFDL model forecast is the Generalized Digital Environmental Model (GDEM) monthly ocean temperature and salinity climatology (Teague et al. 1990), which has ½° horizontal grid spacing and 33 vertical z levels at depths of 0, 10, 20, 30, 50, 75, 100, 125, 150, 200, 250, 300, 400, 500, 600, 700, 800, 900, 1000, 1100, 1200, 1300, 1400, 1500, 1750, 2000, 2500, 3000, 3500, 4000, 4500, 5000, and 5500 m. Other climatologies have been developed since this GDEM version, such as a newer GDEM climatology (more information available online at https://128.160.23.42/gdemv/gdem_desc_v30.html) and a Levitus climatology (Boyer and Levitus 1997) that both have ¼° grid spacing, but tests with these climatologies in the GFDL model do not show increased skill over the original GDEM version used operationally (Yablonsky et al. 2006). The GDEM climatology is then modified by employing an F-B modeling procedure that incorporates observations. This procedure is summarized in sections 2a and 2b and is a major focus of this paper.

After F-B modifications, the upper ocean temperature field is modified by assimilating the real-time daily SST data (with 1° grid spacing) that is used in the operational NCEP Global Forecast System (GFS) global analysis (hereafter NCEP SST; Reynolds and Smith 1994). Next, the three-dimensional temperature and salinity fields are interpolated onto the 23 vertical sigma levels that are used in the subsequent integrations of the Princeton Ocean Model (POM; Blumberg and Mellor 1987; Mellor 2004), which is the ocean component of the GFDL model and currently has ⅙° grid spacing (Bender et al. 2007).[1] POM is subsequently integrated for two days for dynamic adjustment, keeping the SST constant; this ocean model integration is referred to as "phase 1" (FGL05). Then, in "phase 2," the cold wake at the ocean surface and the currents produced by the

[1] The feature-based modeling procedure is not unique to the POM or to the GFDL model as a whole; it can be used to initialize any coupled hurricane forecast model that includes a three-dimensional, primitive equation ocean model.

hurricane prior to the beginning of the coupled model forecast are generated by a three-day integration of POM with the observed hurricane surface wind distribution provided by NOAA's National Hurricane Center (NHC) along the storm track (FGL05). In the present study, all results focus on the ocean temperature field at the end of phase 1; future work may include the impact of F-B data assimilation on the cold wake produced during phase 2 in response to the wind stress from a given hurricane.

Although it is not the focus of this paper, it is instructive to describe the method of SST assimilation, which occurs after F-B modifications are complete, in more detail.[2] First, the OML depth is defined to be the lowest sigma level at which the difference between the preassimilated SST and the temperature at that sigma level is $\leq 0.5°C$. Next, the method of SST assimilation is determined by whether the NCEP SST is (i) greater than or (ii) less than or equal to the preassimilated SST. In scenario (i), the difference between the NCEP SST and the preassimilated SST is added to the preassimilated temperature profile at all sigma levels from the surface to the OML depth. Warming the OML, however, can create an nonphysically large temperature gradient below the OML. Therefore, a transition layer is defined between the OML depth and the level below which no modifications are made to the preassimilated profile. Within the transition layer, which can be as thick as necessary, the temperature is modified to ensure that the vertical temperature gradient does not exceed $0.04°C\ m^{-1}$. In scenario (ii), the preassimilated SST is replaced with the NCEP SST at all levels from the surface down to the level at which the NCEP SST is no longer less than the preassimilated SST. Finally, in both scenarios, convective instability is avoided by forcing any unstable layers in the profile to be convectively neutral.

a. *Overview of the feature-based modeling procedure*

The F-B modeling procedure used as part of the GFDL model ocean initialization is described in detail by FGL05 and references therein. Therefore, only a brief summary of the procedure is presented here, with new improvements described in more detail in the next section. The basic premise of the procedure is that major oceanic fronts in the Atlantic basin, namely the Gulf Stream (GS) and LC, are poorly represented by the GDEM climatology's temperature and salinity fields (e.g., Fig. 1a). By defining the spatial structure of these fronts using historical observations gathered from various field experiments, as discussed in section 3 of FGL05, cross-frontal "sharpening" of the GDEM temperature and salinity fields can be performed to obtain more realistic fields. These sharpened fields yield stronger geostrophically adjusted ocean currents along the front than would be obtained directly from GDEM, causing the former to be more consistent with observations than the latter. In addition, an algorithm was developed to initialize the GS and LC with prescribed paths (see FGL05, their section 4), which may be derived from real-time observations. In the GoM, once

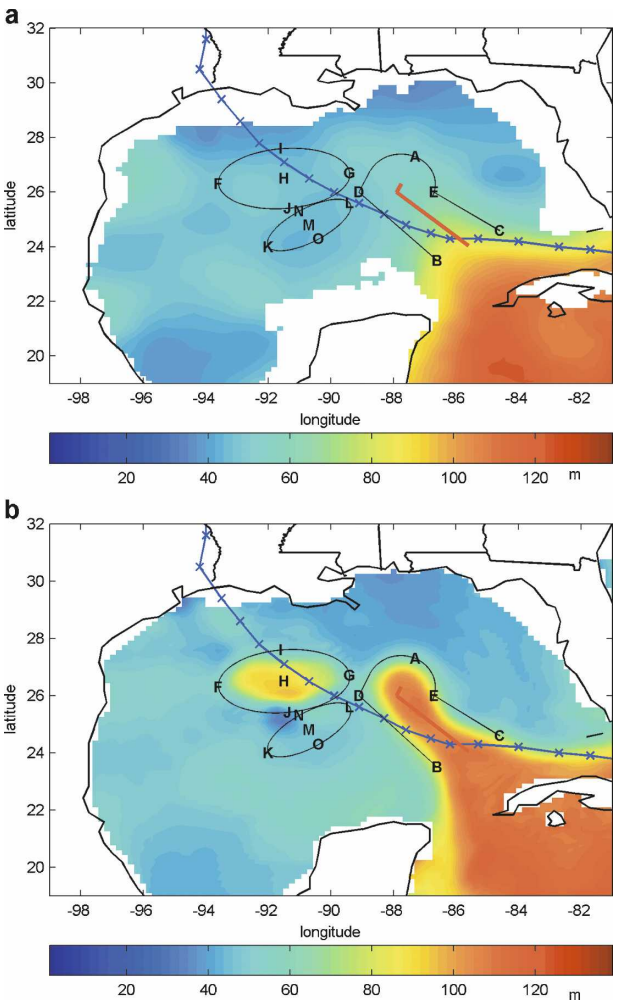

FIG. 1. GoM depth of 26°C isotherm (shaded) (a) in the original GDEM climatology and (b) after 15 Sep 2005 SHA-assimilation. Letters A–E denote points used to construct the LC path. Letters F–J (K–O) denote WCR (CCR) points. Black lines show the constructed LC, WCR, and CCR paths. The red line shows the LC center axis. Hurricane Rita's future track is plotted for reference (blue line with "x" markers).

[2] This method has been used in the operational GFDL model since 2001, but no previous publications describe it. Some modifications were made operational starting in 2006, but these modifications are not used or discussed here.

the LC path is defined, the GDEM temperature profiles along the center line between the into-the-GoM and the out-of the-GoM portion of the LC are replaced with a more accurate temperature profile (hereafter LCPROFILE); by default, the GDEM temperature profile near 21°N, 83°W in the Caribbean Sea is used to define LCPROFILE because the LC water originates from the Caribbean. Cross-frontal sharpening is then performed between these center-line profiles and the surrounding Gulf of Mexico temperature profiles. This version of the LC initialization procedure provides the basis for the new improvements that are described in detail in the next section.

b. *New Loop Current and ring assimilation procedure for the Gulf of Mexico*

In the new ocean initialization procedure, the LC position and structure are more realistically represented, and the ability to initialize LCEs [also known as warm-core rings (WCRs)] and cold-core rings (CCRs) in the GoM has been developed (e.g., Fig. 1b). In FGL05, only the northernmost position of the LC was prescribed. Now, multiple points along the LC path can be specified, allowing the LC shape to be adjusted to match, for example, the observed shape given by near real-time satellite altimetry. In addition, the LC shape can be modified from the form suggested by altimetry (which may not be completely accurate) to a form that is more consistent with near-real-time in situ temperature profiles, when available. Also, the LCPROFILE can be defined based on one or more of these in situ profiles.

LCEs (WCRs) and CCRs are prominent features that typically accompany the LC in the GoM. LCEs rotate anticyclonically in their geostrophically adjusted state because they are warm core and are located from near the ocean surface to ~1000-m depth, below which the horizontal temperature gradient is relatively small and the current velocity is relatively weak. A typical LCE has a diameter of ~200–300 km, a swirl speed of ~1.8–2 m s^{-1}, and a westward translational speed of ~2–5 km day^{-1}. LCEs are formed by eddy shedding of the LC. The physical processes that dictate the irregular time scale of the LC's intrusion into the GoM and eddy shedding (~3–17 months) are not fully understood, but various modeling studies have made major strides toward understanding these processes (Oey et al. 2005 and references therein). Hurlburt and Thompson (1980), for example, conducted sensitivity studies using 1-layer, 1.5-layer reduced-gravity, and 2-layer models and concluded that eddy shedding is caused by horizontal shear instability of the internal mode and requires the planetary β effect for westward spreading of the LC and subsequent eddy separation. Also, the presence of CCRs, which rotate cyclonically in their geostrophically adjusted state (for the same reason LCEs rotate anticyclonically) and typically move clockwise around the periphery of the LC, is hypothesized to play a role in eddy shedding (e.g., Oey et al. 2005; Schmitz 2005). A typical CCR is ~50–150 km in diameter and extends ~1000 m deep (Oey et al. 2005).

In our F-B approach, WCRs and CCRs are assumed to be elliptical in shape (e.g., Fig. 1b), with major and minor axes that can be defined from available observations. Although neither WCRs nor CCRs are perfectly elliptical, this approximation is reasonable based on observations, and in the future, the F-B approach could be improved to allow more variability in the ring shape. The temperature profile at the center of a given WCR (hereafter WCRnPROFILE, where "n" is an integer assigned to the WCR) can be defined based on either (i) a combination of the LCPROFILE, which is assigned a weighting fraction, and the local climatological profile or (ii) near-real-time in situ temperature profile(s). When method (i) is chosen, a 0.8 weighting fraction (where the remaining 0.2 is the local climatological profile) is reasonable based on historical observations, given the assumption that some mixing between the water within the WCR and the surrounding Gulf Common Water (GCW) has occurred since the WCR separated from the LC. Modifying this parameter to be >0.8 or <0.8, however, may be advisable depending on, for example, the size of the WCR and amount of time the WCR has been separated from the LC. For the temperature profile at the center of a given CCR (hereafter CCRnPROFILE), a negative temperature departure from the surrounding climatology (e.g., 2.0°C) can be assigned at a specified depth, currently set to 400 m (i.e., the 13th GDEM level). At the other 32 GDEM levels, the negative temperature departure from climatology is a fraction of the departure at the 13th level. This fraction for each of the 33 GDEM levels is 0, 0, 0, 0, 0, 0, 0.07, 0.15, 0.3, 0.45, 0.6, 0.75, 1, 0.9, 0.8, 0.65, 0.5, 0.35, 0.25, 0.2, 0.1, 0.05, 0.02, 0, 0, 0, 0, 0, 0, 0, 0, 0, and 0, respectively. Therefore, in CCRnPROFILE, the upper 75 m and depths at or below 1500 m are unmodified from climatology during the F-B portion of data assimilation, but recall that the OML and a transition region below the OML are subsequently modified during the SST assimilation phase. Both the 2.0°C departure specified at 400-m depth and the fractions at the other GDEM levels are reasonable based on historical observations, but modifications may be necessary depending on the size and strength of the CCR. Alternatively, the CCRnPROFILE can be defined based on near-real-time in situ temperature profile(s). For both WCRs and

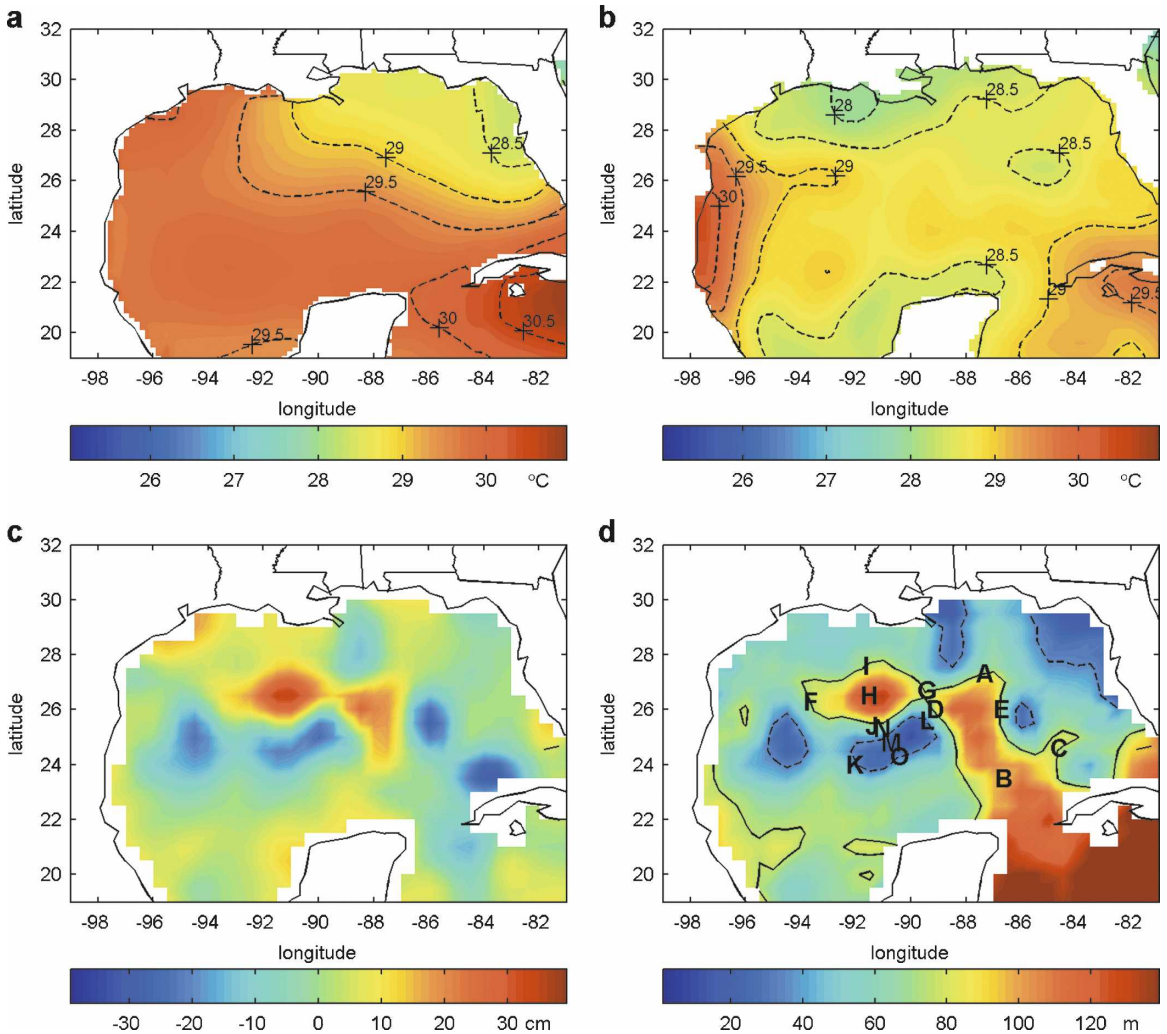

FIG. 2. GoM surface plots: (a) 15 Sep 2005 NCEP SST analysis (shaded and dashed, contour interval 0.5°C); (b) GDEM September climatological SST (shaded and dashed, contour interval 0.5°C); (c) SHA from satellite altimetry (shaded); and (d) depth of 26°C isotherm derived at the NHC from satellite altimetry (shaded), with the 75- and 35-m contour lines plotted (solid and dashed, respectively). Letters A–E denote points used to construct the LC path; letters F–J (K–O) denote WCR (CCR) points.

CCRs, once the ring size and the center profile are defined, cross-frontal sharpening is performed along the elliptical front between the center profile and the surrounding GoM temperature profiles.

3. Evaluation of the new initialization procedure

a. Ocean initialization using 15 September 2005 satellite and in situ data

In advance of Hurricane Rita, on 15 September 2005, 18 AXBTs were deployed successfully in the GoM, providing a unique opportunity to test the capabilities of the initialization procedure described herein. During the winter months, the LC and ring positions are often identifiable from the SST field (e.g., Schmitz 2005). On 15 September 2005, however, the SST is nearly homogeneous in the GoM (Fig. 2a), as is typical during the month of September (Fig. 2b). Therefore, another data source is required. Since the LC contains water originating from the Caribbean Sea, which has a considerably deeper OML base and thermocline than GCW in the GoM, the LC (and associated rings) can be identified from the surrounding GCW by the difference in the dynamic topography (i.e., sea surface height). One suitable data source, therefore, is satellite altimetry (e.g., Leben 2005), from which the daily surface height anomaly (SHA) is currently processed in near–real time (Fig. 2c). The composite SHA product used herein is created at Stennis Space Center in Mississippi by blending multiple ground tracks from any available sat-

ellites [e.g., *Geosat Follow-On* (*GFO*), *Jason-1,* and *Envisat*] and applying appropriate corrections, as described by Mainelli et al. (2008). On and around 15 September 2005, however, only *Jason-1* was functioning and therefore included in the SHA product for that day (M. Mainelli 2007, personal communication).

The altimetric SHA alone is insufficient for monitoring the LC because of the large contribution of the mean circulation to the dynamic topography in the eastern GoM (Leben 2005). To remedy this problem, it is necessary to either (i) have an independent estimate of the long-term altimetric mean sea surface height or (ii) use the SHA to adjust the three-dimensional ocean temperature climatology. Scientists at NHC employ method (ii) by utilizing the Stennis SHA product, a 1.5-layer reduced-gravity ocean model, and a blend of the GDEM and Levitus ocean climatologies to calculate the depth of the 20°C isotherm, the depth of the 26°C isotherm (hereafter d26; Fig. 2d), and the tropical cyclone heat potential (hereafter TCHP; Atlantic Oceanographic and Meteorological Laboratory 2006; Goni et al. 1996)—all of which are currently integrated into the Statistical Hurricane Intensity Prediction Scheme (SHIPS; DeMaria et al. 2005; Mainelli et al. 2008). The TCHP [also commonly referred to as oceanic heat content (OHC)], which is a measure of the integrated heat content from the ocean's surface to d26, provides a quantitative measure of the heat energy available to an approaching tropical cyclone (Leipper and Volgenau 1972; Shay et al. 2000). In the NHC product, the TCHP is calculated by assuming a linear temperature profile between the ocean's surface and d26. Although this method may be reasonable when no additional information is known about the upper ocean profile, the actual TCHP can be more accurately estimated if the structure of the upper ocean profile is known in more detail.

Two cases are run to test the accuracy of the new initialization procedure in the GoM. In the "SHA-assimilated" case, only satellite altimetry (via the 15 September 2005 NHC d26 map) is used to assimilate the LC, a single WCR (hereafter WCR1), and a single CCR (hereafter CCR1) into the GDEM climatology (along with the subsequent assimilation of 15 September 2005 NCEP SST and the two days of POM integration that are part of phase 1). Since no real-time in situ data are assimilated in this case, the results are independent of the 18 real-time AXBTs. In the "fully assimilated" case, however, some of the real-time AXBTs are also used to assimilate the LC, WCR1, and CCR1, so this case is *not* independent of the 18 real-time AXBTs. More details on the SHA-assimilated (fully assimilated) case are given in section 1 (section 2) below.

1) SHA-ASSIMILATED CASE

Using the 15 September 2005 NHC d26 map (Fig. 2d), points A, D, and E along the 75-m contour line are chosen to define the LC path, points F–J (all of which except H are on or near the 75-m contour line) are chosen to define the major and minor axes of an elliptical WCR (i.e., WCR1), and points K–O (all of which except M are on or near the 35-m contour line) are chosen to define the major and minor axes of a CCR (i.e., CCR1). Although choosing points on the 75- and 35-m contour lines is somewhat arbitrary, it allows the perimeter of each feature to be located at or near the region of highest horizontal gradient (i.e., the front), and it removes some of the subjectivity associated with the placement of the features. In reality, point J is slightly south of the 75-m contour line because WCR1 must be constructed as an ellipse, and according to the NHC d26 map, WCR1 is not perfectly elliptical. Similarly, point N is slightly northwest of the 35-m contour line because CCR1 must be constructed as an ellipse, and according to the NHC d26 map, CCR1 is not perfectly elliptical.

The construction of the LC and rings in the assimilation procedure is shown in Figs. 1a and 1b. Starting with the September GDEM climatology (Fig. 1a), point B is defined as the LC position as it enters the GoM from the Caribbean Sea, and point C is defined as the LC position as it exits the GoM and merges with the Florida Current. Due mostly to bathymetric constraints, these two points are generally kept in a fixed "climatological" position regardless of the location of the 75-m contour line on the real-time NHC d26 map. Next, two portions of the LC path are constructed by connecting straight lines between points B and D and between points C and E. The construction of the portion of the LC path north of points D and E is more complex. In Figs. 1a and 1b, only the LC path itself is shown, not the lines used to define the geometry that results in the LC path. In the next paragraph, the geometry that constructs the portion of the LC path north of points D and E is described in more detail.

To construct the LC path north of points D and E, the midpoint between D and E is calculated (hereafter point MDE). Next, a straight line is drawn connecting points MDE and A (hereafter line MDE-A). A line parallel to MDE-A is then drawn that passes through point D (hereafter line MDE-A-PD), and another line parallel to MDE-A is drawn that passes through point E (hereafter line MDE-A-PE). The shortest distance is then found between lines MDE-A and MDE-A-PD (hereafter SD), and a line whose length is equal to SD is drawn from point A toward point MDE (hereafter

line SDL). The southern extent of line SDL is then set to be the center of a circle with radius SD. Next, a semicircle is used to define the LC path, whose orientation is such that the endpoints of the semicircle are tangential to MDE-A-PD and MDE-A-PE. Finally, straight lines connect the endpoints of the semicircle to points D and E, and these straight lines complete the definition of the LC path, as shown in Figs. 1a and 1b.

Once the LC path is defined, the GDEM temperature profiles along the center line between the into-the-GoM and the out-of the-GoM portion of the LC (Figs. 1a and 1b) are replaced with the GDEM temperature profile near 21°N, 83°W in the Caribbean Sea, which in this case is used to define LCPROFILE, after which cross-frontal sharpening is performed with the surrounding GCW, as discussed previously in section 2a. Similarly, the GDEM temperature profile at the center of WCR1 (i.e., point H) is partially replaced with LCPROFILE using the 0.8 fraction to create WCR1PROFILE, and the GDEM temperature profile at the center of CCR1 (i.e., point M) is modified using the 2.0°C negative temperature departure at 400-m depth to create CCR1PROFILE (see previous discussion is section 2b). Just as with the LC, cross-frontal sharpening is performed for the rings with the surrounding GCW, and after both SST assimilation and the 2-day ocean spinup, the resulting d26 (Fig. 1b) is significantly more consistent with the NHC d26 (Fig. 2d) than the original GDEM climatology is (Fig. 1a).

2) FULLY ASSIMILATED CASE

For this case, an attempt was made to achieve more accurate feature identification by subjectively adjusting the LC path and ring size and locations from the form suggested by altimetry based on the available AXBT profiles, whose geographical locations are indicated in Fig. 3a. As will be shown in section 3b, the frontal position of the northwestern part of the LC near the separation point of WCR1 is particularly difficult to determine accurately from altimetry alone, so point D was relocated farther southwest to try to create an LC frontal position that is more accurate at the locations of AXBTs 8–10. Based mostly on AXBTs 11–13, WCR1 was rotated slightly clockwise, contracted slightly along the major axis, expanded slightly along the minor axis, and displaced slightly to the north relative to the SHA-assimilated case (Fig. 3a). Similarly, CCR1 was contracted slightly along the major axis and expanded slightly along the minor axis relative to the SHA-assimilated case. Recall that these modifications are highly subjective, and there are an almost infinite number of possible configurations for the LC and rings, so one could easily argue that agreement with a particular

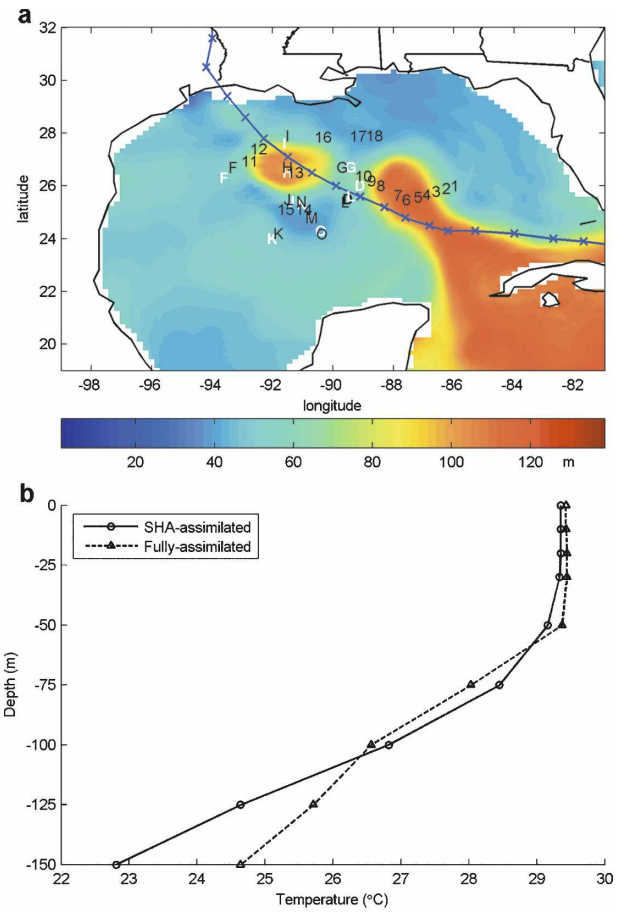

FIG. 3. (a) 15 Sep 2005 fully assimilated GoM depth of 26°C isotherm (shaded). Black letters denote LC, WCR, and CCR points that were changed for the fully assimilated case from the SHA-assimilated case (white letters). Hurricane Rita's future track is again plotted. The 18 AXBT profile locations are indicated by number. (b) SHA-assimilated (solid, circle markers) and fully assimilated (dashed, triangle markers) LCPROFILE.

AXBT or set of AXBTs might be improved by changing the configuration of a given feature slightly one way or another. The main purpose here is to illustrate the potential value of assimilating a limited amount of real-time in situ data if and when such data are available.

In addition to using the AXBT profiles to adjust the configuration of the features, the AXBT 6 profile (instead of the Caribbean profile as in the SHA-assimilated case) is chosen to define the upper 400 m of LCPROFILE for this fully assimilated case because AXBT 6 is located close to the perceived LC center axis. Close examination of the SHA-assimilated and fully assimilated LCPROFILEs (here shown before SST assimilation) reveals that the fully assimilated LCPROFILE is up to ~0.5°C colder than the SHA-assimilated LCPROFILE from the base of the OML

(~55-m depth) down to almost the 26°C level (115-m depth; the difference changes sign at ~105-m depth), but the former is nearly 2°C warmer than the latter at 150-m depth (Fig. 3b). Similarly, the AXBT 13 and 14 profiles are used to define the upper 300 m of WCR1PROFILE and CCR1PROFILE, respectively, in the fully assimilated case. In the future, the AXBT deployment strategy could be improved by dropping a higher concentration of AXBTs close to the perceived LC axis (WCR/CCR center) in an effort to obtain the best possible LCPROFILE (WCR/CCRPROFILE). In the following section (section 3b), results from these SHA-assimilated and fully assimilated simulations are evaluated and compared to another data-assimilated ocean product currently available, RSMAS HYCOM.

b. *Comparison to AXBT profiles and another data-assimilated ocean product (RSMAS HYCOM)*

Assuming the NHC d26 map (Fig. 2d) is reasonably accurate, comparison of either the SHA-assimilated d26 map (Fig. 1b) or the fully assimilated d26 map (Fig. 3a) with the original GDEM climatology (Fig. 1a) reveals that the former estimates the actual LC position and ring locations more accurately than the latter does.[3] To determine whether or not the SHA-assimilated and/or fully assimilated vertical temperature profiles are accurate in the upper ocean, however, it is necessary to compare these profiles to the 18 available AXBT profiles. Also, it is instructive to compare these profiles to concurrent profiles obtained using an alternative data-assimilated ocean product, the daily North and Equatorial Atlantic Ocean Prediction System Best Estimate (hereafter RSMAS HYCOM), which is discussed in the next paragraph.

RSMAS HYCOM is used as an alternative data-assimilated product for comparison purposes. This product is the output from a publicly available version of the HYbrid Coordinate Ocean Model (HYCOM; Chassignet et al. 2005, 2006, 2007). The RSMAS HYCOM dataset from 15 September 2005 was downloaded from the University of Miami's HYCOM consortium data server Web site (http://hycom.rsmas.miami.edu/dataserver). RSMAS HYCOM employs an Optimal Interpolation (OI) technique with Cooper and Haines (1996) for downward projection of the Modular Ocean Data Assimilation System (MODAS) daily sea surface height analysis (Fox et al. 2002), which is derived from satellite altimetry (Chassignet et al. 2007). In addition, the RSMAS HYCOM model SST is relaxed to the MODAS ⅛° SST analysis (Chassignet et al. 2007). To the authors' knowledge, no in situ data are assimilated into the RSMAS HYCOM product used herein.

All GDEM, SHA-assimilated, fully assimilated, and RSMAS HYCOM temperature profiles are bilinearally interpolated to each AXBT profile's location. Visual analysis of these temperature profiles allows for comparison of individual aspects of the profile (e.g., mixed layer temperature and depth, upper thermocline temperature, vertical temperature gradient, etc.), but conclusions drawn from such an analysis are necessarily subjective. Calculation of the TCHP provides a quantitative measure of the accuracy of each profile. Recall, however, that TCHP is a measure of the oceanic heat content integrated from the surface to d26; two temperature profiles with the same TCHP may experience differing degrees of SST cooling due to hurricane wind stress if the shapes of the two profiles are different. Therefore, TCHP comparisons can supplement but should not replace analysis of the vertical temperature profile shape. In section 3b(1), the temperature profiles are compared individually, and only the upper 150 m of the ocean is examined. In the section 3b(2), the TCHP is examined.

1) PROFILE COMPARISON

AXBT 1 is located outside of the eastern branch of the LC (Fig. 3a). According to Fig. 4a, the initial GDEM climatology has an OML that is ~0.5°C too cold and an upper thermocline (i.e., above 150-m depth) that is ~2°–3°C too warm. After SHA or full assimilation, however, the OML temperature is nearly identical to the AXBT OML temperature, and the upper thermocline is only ~1°–2°C too warm. In all three cases, the OML depth is ~10 m too shallow, but this error may be due to the relatively coarse vertical resolution in the climatology (i.e., no levels between 30- and 50-m depth; see section 2). By comparison, the RSMAS HYCOM OML is nearly identical to the GDEM climatology OML (i.e., ~0.5°C too cold relative to the AXBT OML), and although the RSMAS HYCOM extreme upper thermocline (~50–70-m depth) is quite accurate, the vertical temperature gradient below 70 m is too large, so the temperature at >80-m depth is ~3°C too cold. Finally, note that full assimilation yields an upper thermocline that is up to ~0.5°C warmer than SHA assimilation, but this small extra error may be worth the increased accuracy obtained on the northwest side of the LC using full assimilation, as discussed later in this section.

[3] The date 15 September 2005 is one week before Hurricane Rita traversed the GoM and made landfall near the Texas–Louisiana border. For reference, Rita's track is plotted to show the hurricane's proximity to the LC and rings.

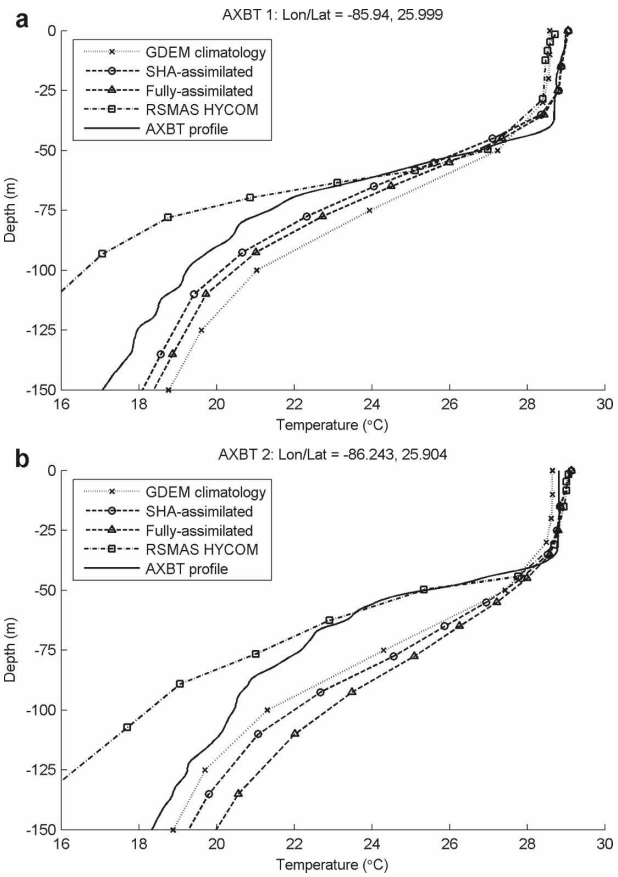

FIG. 4. GDEM September climatology (dotted, "x" markers), SHA-assimilated profile (dashed, circle markers), fully assimilated profile (dashed, triangle markers), RSMAS HYCOM profile (dot-dashed, square markers), and AXBT temperature profile (solid) for (a) AXBT 1 and (b) AXBT 2. AXBT positions are given at the top of each panel; see Fig. 3a for location in the GoM basin.

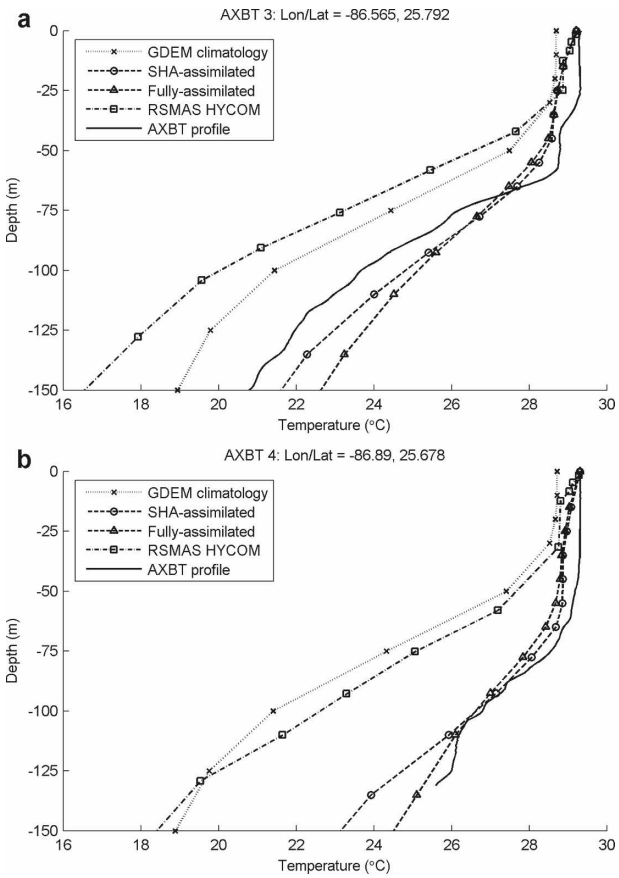

FIG. 5. Same as Fig. 4, but for AXBT (a) 3 and (b) 4.

AXBTs 2–5 progressively approach the LC center line along a path that begins with AXBT 1 and ends near the center line between the two LC branches (Fig. 3a). For AXBT 2 (Fig. 4b), the climatological, SHA-assimilated, and fully assimilated OMLs are accurate, but the upper thermocline is too warm because the temperature gradient at the base of the OML is too gradual. The RSMAS HYCOM OML is also accurate, as is the temperature in the extreme upper thermocline (~40–70-m depth), but again the vertical temperature gradient below 70 m is too large, so the temperature at >70-m depth is too cold. For AXBT 3 (Fig. 5a), the climatological profile from the surface to 150-m depth is too cold. SHA assimilation and full assimilation both improve the profile from climatology, but the OML is still slightly too shallow and cold, and the gradual temperature gradient at the base of the OML causes the temperature below 70-m depth to be up to ~1°C (~2°C) too warm in the SHA-assimilated (fully assimilated) case. The RSMAS HYCOM OML is similar to climatology (too cold and shallow), and the temperature below the OML is even colder than climatology. For AXBT 4 (Fig. 5b), climatology and RSMAS HYCOM are similar to each other, but both are up to 6°C too cold in the upper thermocline. SHA assimilation and full assimilation, however, improve the profile dramatically from climatology, creating an accurate OML depth and upper thermocline temperature. Unfortunately, AXBT 4 only functioned down to 131-m depth, but at this level, the advantage of full assimilation over SHA assimilation first becomes apparent, as the former is ~1°C more accurate than the latter. For AXBT 5 (Fig. 6a), climatology is again up to 6°C too cold in the upper thermocline, while RSMAS HYCOM is up to 5°C too cold in the upper thermocline. SHA assimilation produces a relatively accurate profile, but the upper thermocline temperature is up to 2°C too cold below ~100-m depth. The fully assimilated profile, however, is nearly identical to the AXBT profile.

AXBTs 6–10 progressively approach the northwestern edge of a path that begins near the LC center line

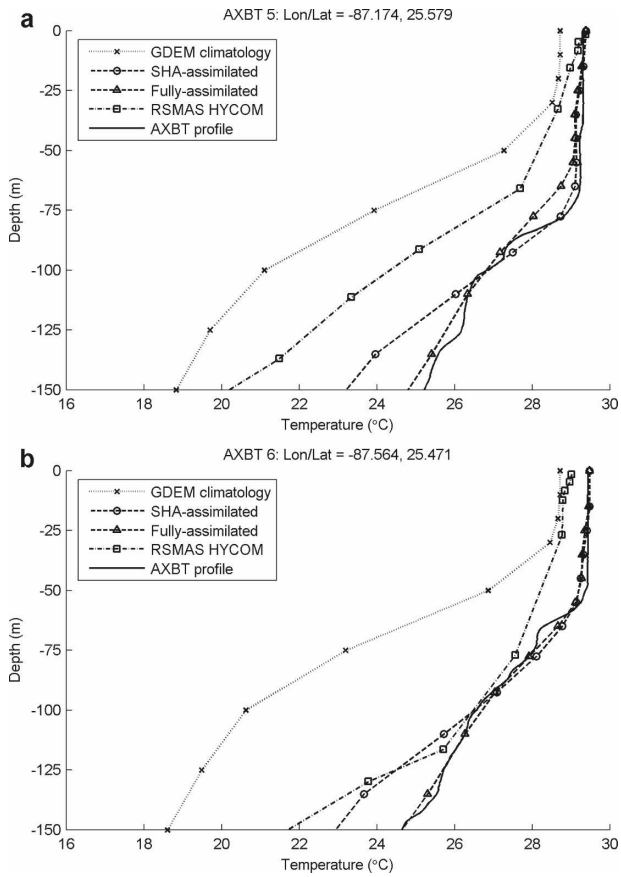

FIG. 6. Same as Fig. 4, but for AXBT (a) 5 and (b) 6.

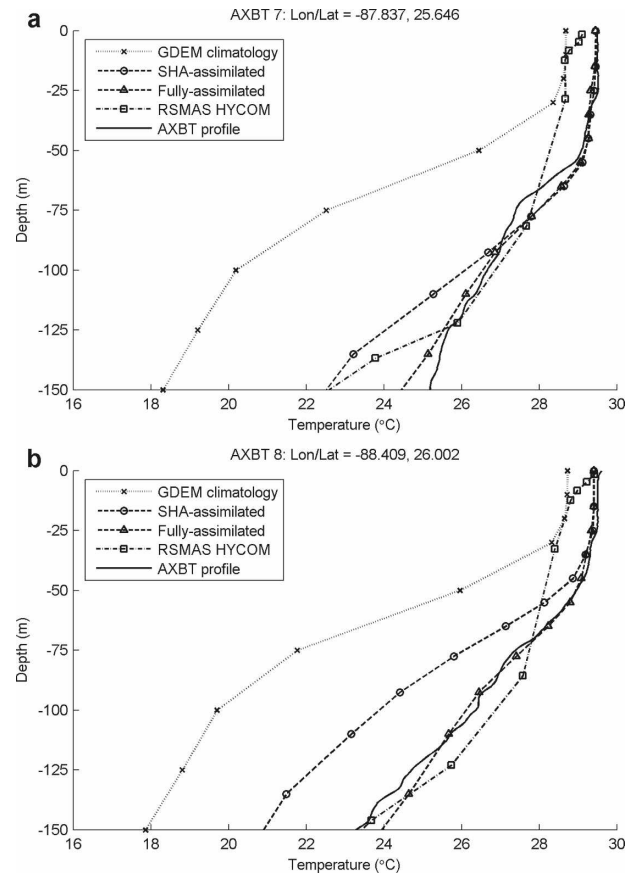

FIG. 7. Same as Fig. 4, but for AXBT (a) 7 and (b) 8.

and ends near the northwestern periphery of the LC (Fig. 3a). For AXBT 6 (Fig. 6b), which is used to define the upper 400-m of LCPROFILE in the fully assimilated case, climatology is up to 6°C too cold in the upper thermocline. SHA assimilation yields an accurate OML depth and temperature, but the temperature gradient is slightly too gradual at the OML base and slightly too large below this level, resulting in a temperature that is up to nearly 2°C too cold below ~100-m depth. Not surprisingly, the fully assimilated profile is nearly identical to the AXBT profile. RSMAS HYCOM's OML depth is relatively accurate, but the temperature is 1°C too cold, and poor vertical resolution inhibits proper representation of the OML base. At 150-m depth, RSMAS HYCOM is ~3°C too cold. For AXBT 7 (Fig. 7a), the results are similar to AXBT 6, except neither the SHA-assimilated nor the fully assimilated profile can capture the locally sharp temperature gradient in the ~60–75-m depth layer. For both AXBT 8 (Fig. 7b) and 9 (Fig. 8a), the potential improvement afforded by using real-time AXBTs to restructure the LC path becomes most apparent. While the SHA-assimilated profiles are up to ~3°C too cold throughout the upper thermocline at both of these AXBT locations, the fully assimilated profiles are generally within ~1°C of their respective AXBT profiles, except locally at the base of the OML for AXBT 9. RSMAS HYCOM is ~1°C too cold in the OML and ~1°C too warm below 75-m depth for both of these AXBTs. For AXBT 10 (Fig. 8b), climatology is up to 4°C too cold in the upper thermocline. SHA assimilation and full assimilation both yield an OML that is slightly too deep, but the former (latter) yields an upper thermocline temperature that is ~0.5°C (~1°C) too cold (warm). RSMAS HYCOM's upper thermocline temperature is ~3°C too warm.

AXBTs 11 and 12 are located near the northwestern edge of an LCE (i.e., WCR1), and AXBT 13 (used to define the upper 300 m of WCR1PROFILE) is located near the center of that LCE (Fig. 3a). For AXBT 11 (Fig. 9a), climatology is up to 6°C too cold in the upper thermocline. SHA and full assimilation improve the climatological profile so that the upper thermocline is at most 2°C too cold. RSMAS HYCOM yields an OML depth that is slightly too deep and a temperature gradient in the upper thermocline that is too large, yielding

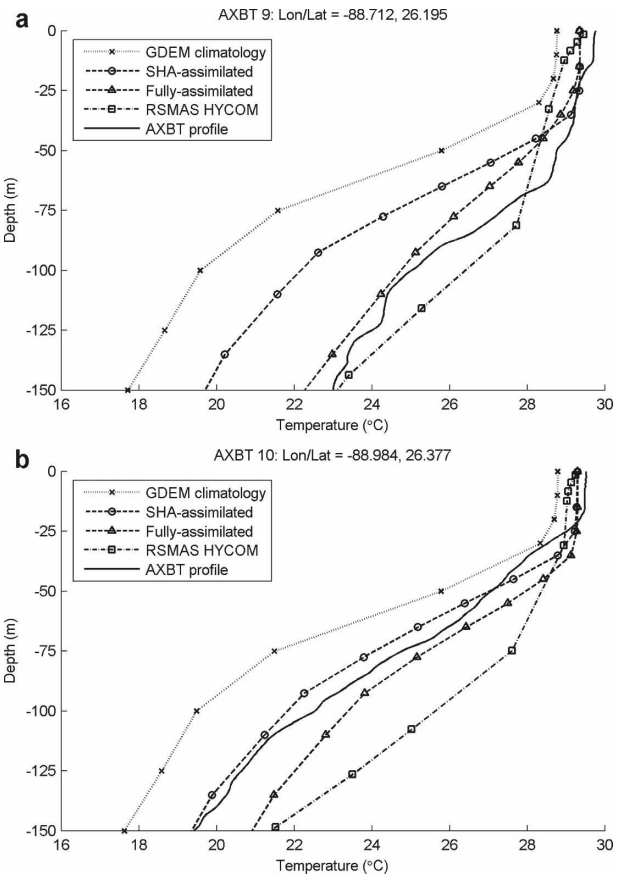

FIG. 8. Same as Fig. 4, but for AXBT (a) 9 and (b) 10.

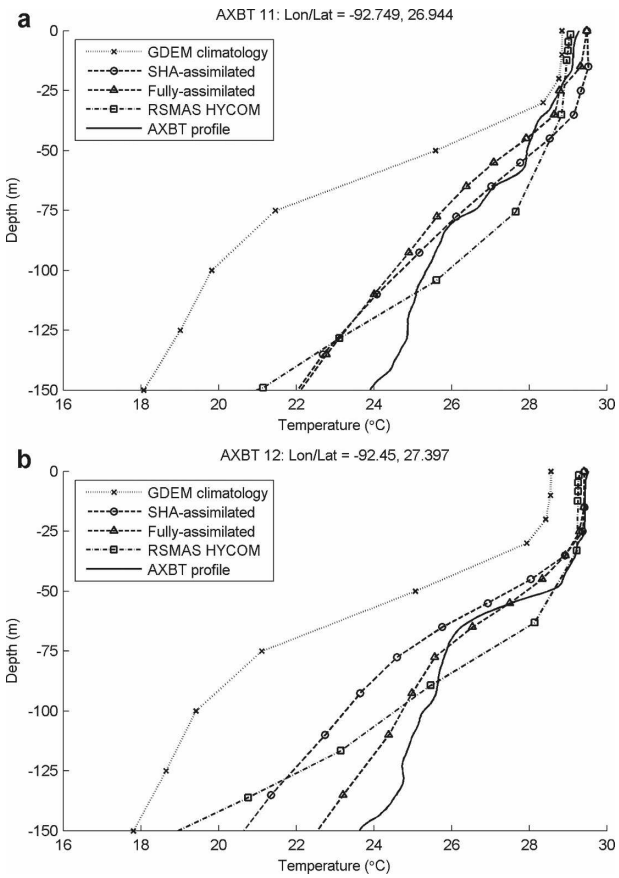

FIG. 9. Same as Fig. 4, but for AXBT (a) 11 and (b) 12.

a profile that is up to 2°C too warm above 110-m depth and up to 3°C too cold below 110-m depth. For AXBT 12 (Fig. 9b), the results are similar to AXBT 11, but here the fully assimilated profile is significantly more accurate than the SHA-assimilated profile below ~75-m depth. Also, the large RSMAS HYCOM temperature gradient in the upper thermocline renders that profile less accurate (>4°C too cold at 150-m depth). For AXBT 13 (Fig. 10a), climatology is again up to 6°C too cold in the upper thermocline. SHA assimilation is ~2°C too cold, while full assimilation is <1°C too cold, although both of these profiles have an OML depth that is ~10 m too shallow. RSMAS HYCOM is similar to the SHA-assimilated profile, except the upper thermocline temperature is up to 2°C too cold.

AXBTs 14 and 15 are located in a CCR (i.e., CCR1) to the south of the aforementioned LCE (Fig. 3a). For AXBT 14 (used to define the upper 300 m of CCR1PROFILE) (Fig. 10b), climatology has an OML that is too cold and deep and an upper thermocline that is up to 5°C too warm. SHA assimilation and full assimilation improve the OML temperature, but the OML is still too deep in the fully assimilated case. In regards to the upper thermocline, the fully assimilated profile is able to capture the sharp vertical temperature gradient better than either the SHA-assimilated profile or climatology is. RSMAS HYCOM has a submerged OML located below an unsubstantiated temperature gradient near the surface and an upper thermocline temperature that is too warm. For AXBT 15 (Fig. 11a), climatology again has an OML that is too cold, but the upper thermocline is only ~1°C too warm. SHA assimilation and especially full assimilation yield an even more accurate profile. RSMAS HYCOM has an OML that is slightly too cold, a temperature in the ~30–70-m depth layer that is ~2°C too warm, and a temperature below 70-m depth that is ~2°C too cold.

AXBTs 16–18 are located near the southeastern Louisiana coastline, north of the LC and LCE (Fig. 3a). For AXBT 16 (Fig. 11b), climatology has an OML that is too shallow and an upper thermocline temperature that is up to ~2°C too cold. SHA assimilation and especially full assimilation improve the upper thermocline temperature, but the OML is still too shallow in both cases. RSMAS HYCOM has an OML that is too warm and shallow and a sharp temperature gradi-

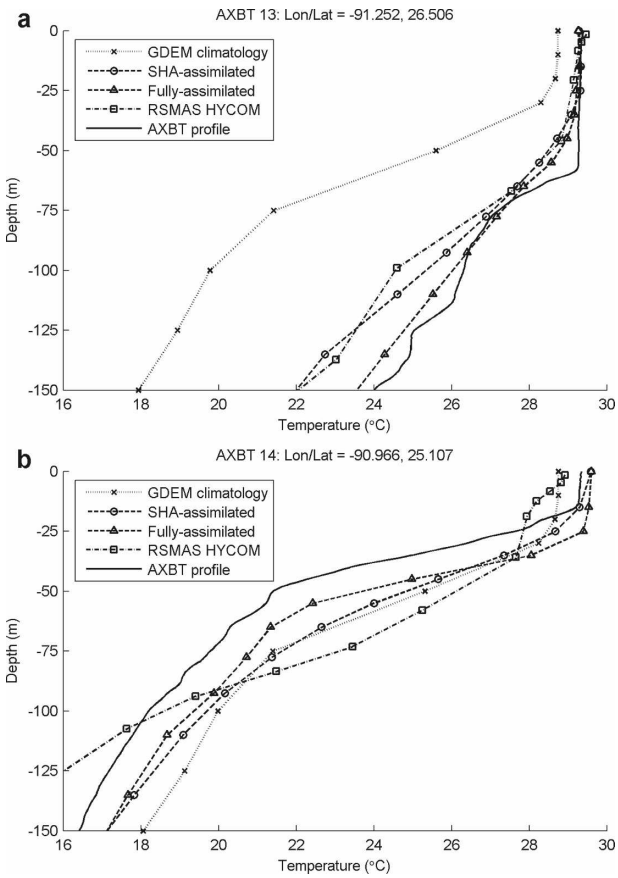

FIG. 10. Same as Fig. 4, but for AXBT (a) 13 and (b) 14.

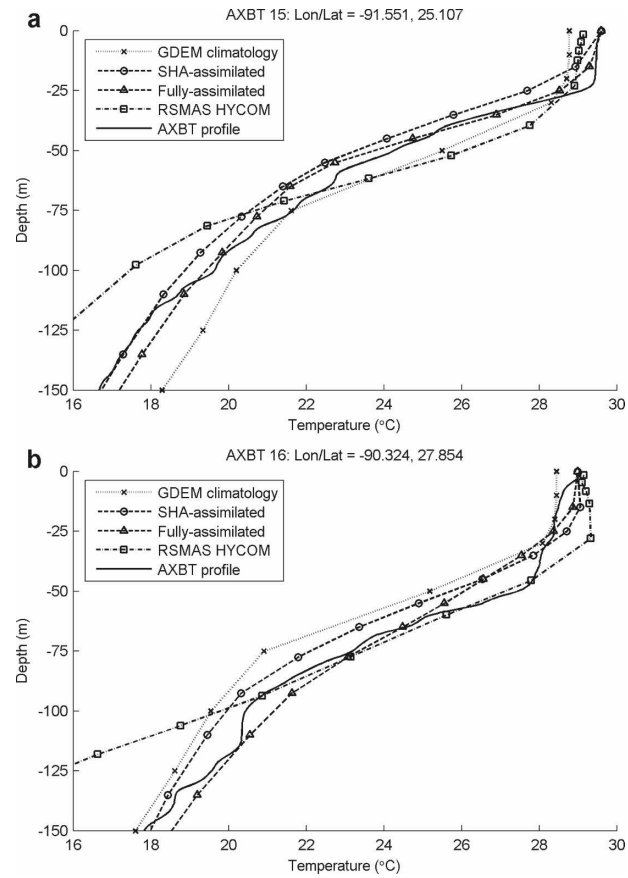

FIG. 11. Same as Fig. 4, but for AXBT (a) 15 and (b) 16.

ent in the upper thermocline that causes the profile to become too cold below ~95-m depth. For AXBT 17 (Fig. 12a), climatology is accurate from the surface to ~65-m depth and is slightly too cold below this depth. Interestingly, SHA initialization and full assimilation both slightly degrade the profile by making it up to ~1°C colder than climatology in the upper thermocline. RSMAS HYCOM's OML is far too deep and warm (up to 4°C), and the temperature gradient in the upper thermocline is again too large, yielding a temperature at ~110-m depth that is nearly 5°C too cold. For AXBT 18 (Fig. 12b), the results are similar to AXBT 17, but the difference between the SHA-fully assimilated and AXBT profiles is greater while the difference between the RSMAS HYCOM and AXBT profiles is less. The exact reason(s) for the slight degradation (i.e., anomalous cooling) of the profiles after SHA or full assimilation at the locations of AXBTs 17 and 18 is debatable. Part of the degradation occurs after sharpening and SST assimilation and during the 2-day spinup (not shown). This part could be explained by upwelling that occurs within a CCR that develops northwest of the LC and northeast of the WCR1 in response to the placement and shape of these latter two features. The rest of the cooling occurs during the sharpening of the LC, so further testing with additional in situ data (when available) and perhaps future modifications to the sharpening procedure may be required to prevent such degradation.

2) TCHP COMPARISON

Figure 13 presents the TCHP calculated at each AXBT location (i) from the GDEM climatology, (ii) after SHA assimilation, (iii) after full assimilation, (iv) from RSMAS HYCOM, and (v) from the AXBT itself. At both locations east of the LC (i.e., AXBTs 1 and 2), all five TCHP values are within ~13 kJ cm^{-2} of each other. Inside the LC (i.e., AXBT locations 3–9), the differences increase dramatically. The GDEM values inside the LC remain between 43 and 52 kJ cm^{-2}. SHA assimilation, however, yields values inside the LC as high as 125 kJ cm^{-2}, which is supported by the AXBT profiles (e.g., AXBT 5 TCHP = 128 kJ cm^{-2}). Fully assimilated values inside the LC are generally within ~10 kJ cm^{-2} of the corresponding SHA-assimilated value, except for AXBT 8, for which the fully assimi-

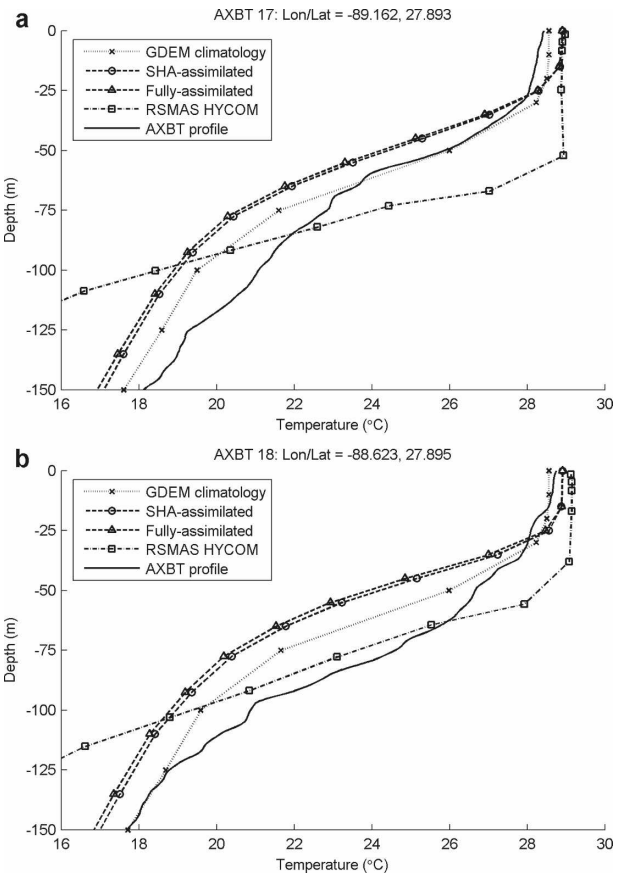

FIG. 12. Same as Fig. 4, but for AXBT (a) 17 and (b) 18.

lated TCHP is significantly higher (and more accurate) than the SHA-assimilated TCHP. This difference is due to the reorientation of the northwestern part of the LC path in the fully assimilated case versus the SHA-assimilated case. RSMAS HYCOM yields LC values as high as 106 kJ cm^{-2}, but this maximum occurs farther west than the AXBTs and the SHA and fully assimilated profiles suggest. Considering now AXBT locations 11–13, which include WCR1, it is apparent that the TCHP has only one peak in RSMAS HYCOM, whereas the AXBT and the SHA and fully assimilated TCHP values are bimodal. Focusing on RSMAS HYCOM's overestimate of TCHP at the location of AXBT 10 suggests that RSMAS HYCOM fails to adequately separate WCR1 from the LC. In fact, while the SHA-assimilated TCHP reveals a coherent LC and ring structure (Fig. 14a), RSMAS HYCOM indicates a more complex spatial variation of TCHP in the GoM (Fig. 14b).

Recall that AXBTs 14 and 15 are located in CCR1. Although neither of these AXBTs is near the center of CCR1, AXBT 14 is used as CCR1PROFILE in the fully assimilated case because it is the best data available (other than, arguably, not using any AXBTs for CCR1PROFILE, as in the SHA-assimilated case). Hence, the fully assimilated profile overestimates the TCHP at the location of AXBT 14 by ~18 kJ cm^{-2}, whereas the GDEM climatology and RSMAS HYCOM only overestimate the TCHP at this location by ~7 kJ cm^{-2}. Although the RSMAS HYCOM TCHP is more accurate than either the SHA-assimilated or the fully assimilated TCHP at this location, recall that the shape of the RSMAS HYCOM profile is inconsistent with the shape suggested by the AXBT (Fig. 10b). To decrease the fully assimilated TCHP at the location of AXBT 14, CCR1PROFILE could be adjusted by decreasing the upper ocean temperature at each level by a specified amount during the data-assimilation phase.

In the northern GoM off the southeastern Louisiana coast (i.e., the location of AXBTs 16–18), RSMAS HYCOM overestimates the TCHP. In the case of AXBT 17, RSMAS HYCOM's TCHP is 46 kJ cm^{-2} too large; in contrast, GDEM's TCHP, the SHA-assimilated TCHP, and the fully assimilated TCHP are only 5, 1, and 0 kJ cm^{-2} too large, respectively. Further investigation is needed to determine why RSMAS HYCOM overestimates the TCHP in this region and whether this result is case specific or systematic. Figure 14b reveals that this RSMAS HYCOM TCHP overestimate may be due to a spurious small-scale WCR that is partially attached to the northern end of a poorly defined LC.

To obtain a crude but concise picture of the overall error associated with each initialization technique in the GoM, it is helpful to calculate the TCHP rms error based on the temperature profiles at all 18 AXBT locations. Taking the AXBT profiles to be truth, the TCHP rms error associated with the GDEM climatology, SHA assimilation, full assimilation, and RSMAS HYCOM is 45, 12, 10, and 26 kJ cm^{-2}, respectively. Thus, the SHA-assimilated and fully assimilated simulations provide considerably more accurate initialization of the main mesoscale features in the GoM than either the GDEM climatology or RSMAS HYCOM does.

4. Summary and conclusions

Using an F-B modeling approach that assimilates satellite-derived SHA, SST, and in situ data in the GoM, a new ocean initialization has been developed for the GFDL/URI coupled hurricane–ocean model. This new procedure is designed to account for spatial and temporal variability of mesoscale oceanic features in the Gulf of Mexico, including the LC, LCEs (WCRs), and CCRs. Using near-real-time satellite altimetry and, in the fully assimilated case only, in situ temperature profiles, these features are assimilated into the original cli-

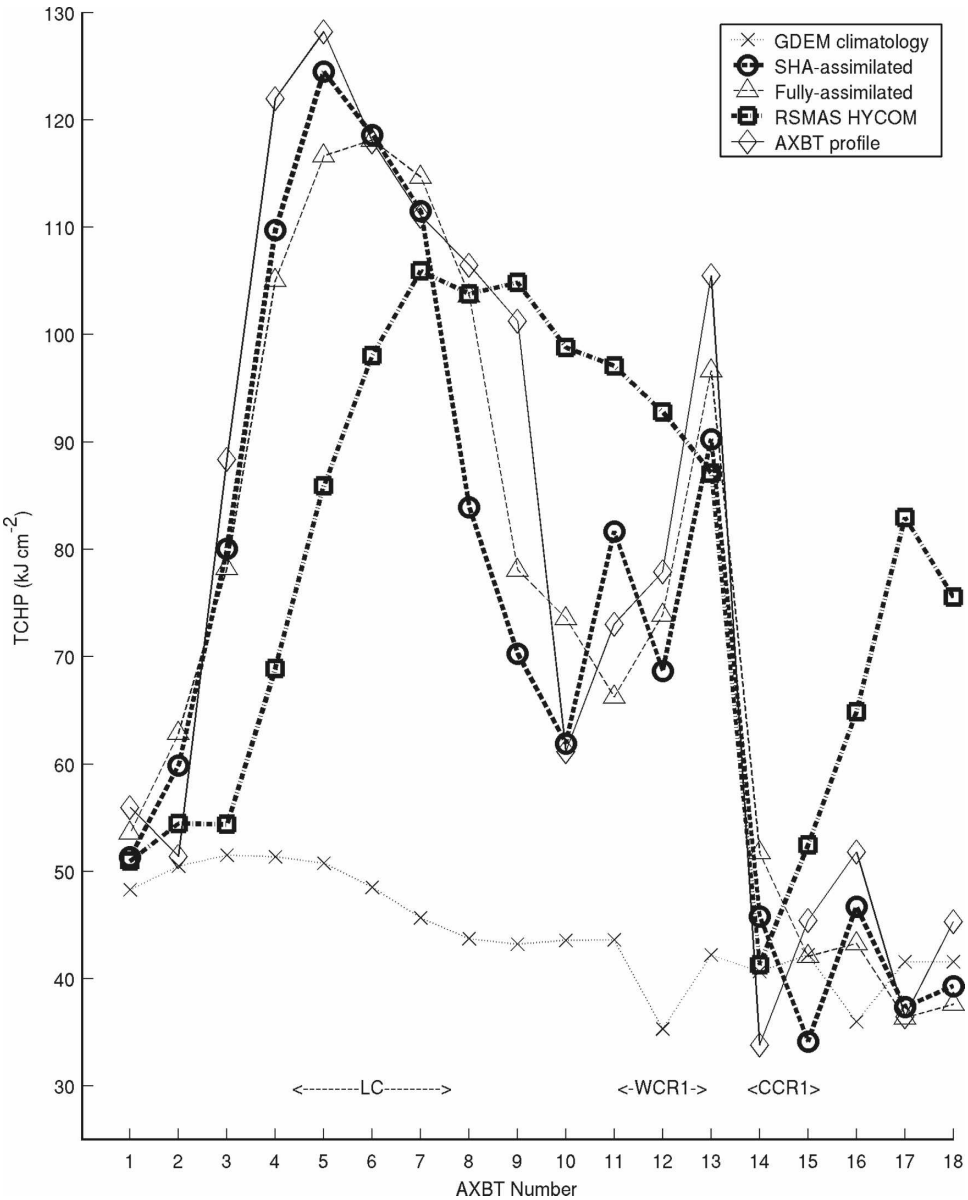

FIG. 13. TCHP at each AXBT location based on the GDEM September climatology (dotted, "x" markers), SHA-assimilated profile (bold dashed, circle markers), fully assimilated profile (dashed, triangle markers), RSMAS HYCOM profile (bold dotted–dashed, square markers), and AXBT profile (solid, diamond markers).

matology to produce a more realistic three-dimensional temperature field valid at the model initialization time. Vertical profiles from the resulting F-B data-assimilated temperature fields are compared to 18 AXBT temperature profiles on 15 September 2005, the ocean climatology, and an alternative data-assimilated product (RSMAS HYCOM) to determine the relative accuracy of the initialization procedure presented here. Also, the TCHP from each of these profiles is calculated.

The F-B ocean initialization creates a significantly improved three-dimensional temperature field over climatology. Also, when evaluating OML temperature and depth and upper thermocline temperature against 18 GoM AXBT profiles, this initialization technique is more accurate than a best estimate of the three-dimensional ocean temperature obtained using an alternative data-assimilated product (i.e., RSMAS HYCOM). Calculation of the TCHP and the TCHP rms error supports this conclusion and suggests that the ini-

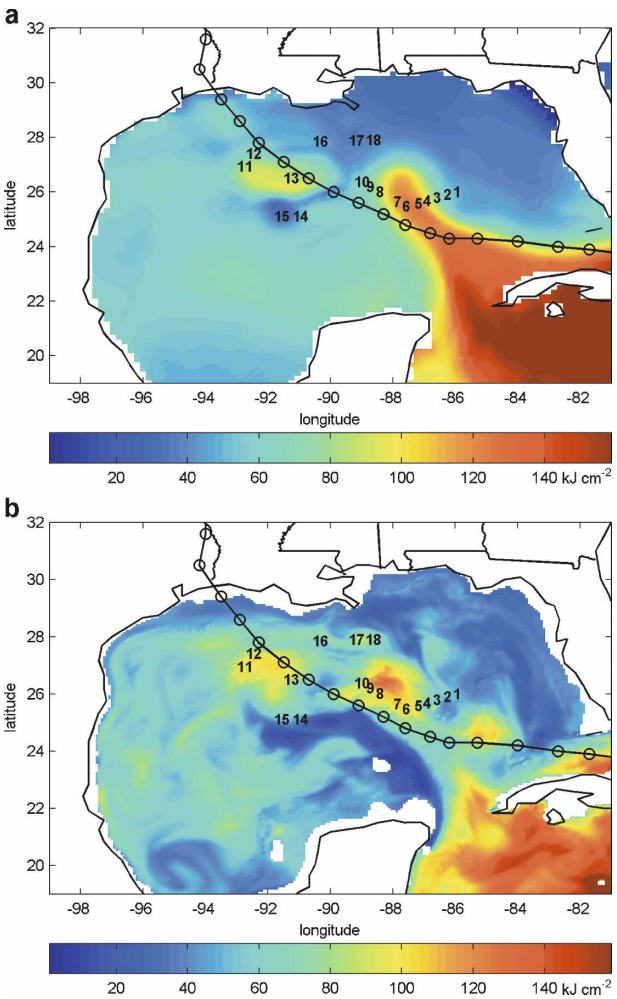

FIG. 14. GoM TCHP (shaded and dashed, contour interval 20 kJ cm^{-2}) (a) after SHA-assimilation and (b) in RSMAS HYCOM. The 18 AXBT profile locations are indicated again by number, and Hurricane Rita's future track is plotted for reference.

tialization technique presented here is particularly superior to the RSMAS HYCOM product in the northern GoM and wherever a LCE may be separating from (or reattaching to) the LC. In the latter case, the ability to manually adjust the position of the features based on near-real-time AXBT profiles rather than relying exclusively on satellite altimetry is particularly advantageous. It is hoped that these new improvements to the three-dimensional temperature of the LC and associated rings will improve hurricane intensity prediction in the GoM.

Unfortunately, not all of the initialization improvements discussed here were ready before the deadline for incorporation into the 2006 operational GFDL model. Some of the improvements were incorporated though, including the ability to define multiple points along the LC path and to define a single elliptical WCR. During the 2006 and 2007 hurricane seasons, forecasters at NHC used d26 maps derived from satellite altimetry (see section 3) to define LC and WCR parameters for initialization of the GFDL model operational forecasts. No changes were made to the GFDL model's ocean initialization between the 2006 and 2007 hurricane seasons.

In early 2007, the ocean component of the GFDL/URI coupled model, POM, was coupled to NCEP's Hurricane Weather Research and Forecasting (WRF) atmospheric model. The 2006/07 GFDL model ocean initialization was transitioned directly into this new coupled version of the Hurricane WRF model, which subsequently became operational at NCEP before the start of the 2007 hurricane season. This initialization procedure can be easily adapted to work with the ocean component of other coupled models as well, regardless of whether or not that ocean component is POM. Also, the initialization procedure is currently in the process of being partially automated so that, for example, a specified contour line on a GoM d26 map (e.g., 75 m) or sea surface height map (e.g., 17 cm) can be used to automatically provide a first guess of the LC and WCR positions (e.g., Leben 2005), after which the positions can be automatically adjusted based on any available in situ ocean temperature profiles with minimal human input.

Acknowledgments. The authors first wish to thank Aleksandr Falkovich for providing the F-B model and Eric Uhlhorn for providing the processed AXBT profiles. Next, we thank Michelle Mainelli and Stephen Baig for the processed SHA, d26, and TCHP data and for updating the GFDL model ocean initialization parameters in near–real time during the 2006 and 2007 hurricane seasons. We also thank the HYCOM Consortium (RSMAS) for providing RSMAS HYCOM model output. Special thanks to all of the research members of the URI/GSO Numerical Modeling Lab for technical assistance and helpful suggestions. This research was funded by both SAIC/NOAA/NCEP Grant 4400080656 and KORDI Grant PG45100, awarded to the Graduate School of Oceanography at URI, and a URI Distinguished Graduate Student Fellowship in Physical Oceanography, awarded to the first author.

REFERENCES

Atlantic Oceanographic and Meteorological Laboratory, cited 2006: Tropical cyclone heat potential. [Available online at http://www.aoml.noaa.gov/phod/cyclone/data/gl.html.]

Bender, M. A., and I. Ginis, 2000: Real-case simulation of hurri-

cane–ocean interaction using a high-resolution coupled model: Effects on hurricane intensity. *Mon. Wea. Rev.,* **128,** 917–946.

——, ——, R. Tuleya, B. Thomas, and T. Marchok, 2007: The operational GFDL Coupled Hurricane–Ocean Prediction System and summary of its performance. *Mon. Wea. Rev.,* **135,** 3969–3989.

Blumberg, A. F., and G. L. Mellor, 1987: A description of a three-dimensional coastal ocean circulation model. *Three-Dimensional Coastal Ocean Models.* N. Heaps, Ed., Vol. 4, Amer. Geophys. Union, 1–16.

Boyer, T. P., and S. Levitus, 1997: *Objective Analysis of Temperature and Salinity for the World Ocean on a ¼ Grid.* NOAA Atlas NESDIS 11, 62 pp.

Chassignet, E. P., and Coauthors, 2005: Assessment of data assimilative ocean models in the Gulf of Mexico using ocean color. *Circulation in the Gulf of Mexico: Observations and Models, Geophys. Monogr.,* Vol. 161, Amer. Geophys. Union, 87–100.

——, H. E. Hurlburt, O. M. Smedstad, G. R. Halliwell, P. J. Hogan, A. J. Wallcraft, and R. Bleck, 2006: Ocean prediction with the HYbrid Coordinate Ocean Model (HYCOM). *Ocean Weather Forecasting: An Integrated View of Oceanography,* E. P. Chassignet and J. Verron, Eds., Springer, 413–426.

——, ——, ——, ——, ——, ——, R. Baraille, and R. Bleck, 2007: The HYCOM (HYbrid Coordinate Ocean Model) data assimilative system. *J. Mar. Syst.,* **65,** 60–83.

Cione, J. J., and E. W. Uhlhorn, 2003: Sea surface temperature variability in hurricanes: Implications with respect to intensity change. *Mon. Wea. Rev.,* **131,** 1783–1796.

Cooper, M., and K. Haines, 1996: Altimetric assimilation with water property conservation. *J. Geophys. Res.,* **101,** 1059–1078.

DeMaria, M., M. Mainelli, L. K. Shay, J. A. Knaff, and J. Kaplan, 2005: Further improvements to the Statistical Hurricane Intensity Prediction Scheme (SHIPS). *Wea. Forecasting,* **20,** 531–543.

Emanuel, K. A., 1986: An air–sea interaction theory for tropical cyclones. Part I: Steady-state maintenance. *J. Atmos. Sci.,* **43,** 585–604.

——, 1999: Thermodynamic control of hurricane intensity. *Nature,* **401,** 665–669.

Falkovich, A., I. Ginis, and S. Lord, 2005: Ocean data assimilation and initialization procedure for the Coupled GFDL/URI Hurricane Prediction System. *J. Atmos. Oceanic Technol.,* **22,** 1918–1932.

Fox, D. N., W. J. Teague, C. N. Barron, M. R. Carnes, and C. M. Lee, 2002: The Modular Ocean Data Assimilation System (MODAS). *J. Atmos. Oceanic Technol.,* **19,** 240–252.

Ginis, I., 2002: Tropical cyclone–ocean interactions. *Atmosphere–Ocean Interactions,* W. Perrie, Ed., Advances in Fluid Mechanics Series, Vol. I, No. 33, WIT Press, 83–114.

Goni, G., and J. Trinanes, 2003: Ocean thermal structure monitoring could aid in the intensity forecast of tropical cyclones. *Eos, Trans. Amer. Geophys. Union,* **84,** 573–580.

——, S. Kamholz, S. Garzoli, and D. Olson, 1996: Dynamics of the Brazil–Malvinas confluence based on inverted echo sounders and altimetry. *J. Geophys. Res.,* **101,** 16 273–16 289.

——, P. Black, and J. Trinanes, 2003: Using satellite altimetry to identify regions of hurricane intensification. *AVISO Newsletter,* Vol. 9, AVISO, Ramonville St. Agne, France, 19–20.

Hurlburt, H. E., and J. D. Thompson, 1980: A numerical study of Loop Current intrusions and eddy shedding. *J. Phys. Oceanogr.,* **10,** 1611–1651.

Leben, R. R., 2005: Altimeter-derived Loop Current metrics. *Circulation in the Gulf of Mexico: Observations and Models, Geophys. Monogr.,* Vol. 161, Amer. Geophys. Union, 181–201.

Leipper, D., and D. Volgenau, 1972: Hurricane heat potential of the Gulf of Mexico. *J. Phys. Oceanogr.,* **2,** 218–224.

Mainelli, M., M. DeMaria, L. K. Shay, and G. Goni, 2008: Application of oceanic heat content estimation to operational forecasting of recent Atlantic category 5 hurricanes. *Wea. Forecasting,* **23,** 3–16.

Mellor, G. L., 2004: User's guide for a three-dimensional, primitive equation, numerical ocean model (June 2004 version). Tech. Rep., Program in Atmospheric and Ocean Sciences, Princeton University, 56 pp.

Oey, L.-Y., T. Ezer, and H.-C. Lee, 2005: Loop Current, rings, and related circulation in the Gulf of Mexico: A review of numerical models and future challenges. *Circulation in the Gulf of Mexico: Observations and Models, Geophys. Monogr.,* Vol. 161, Amer. Geophys. Union, 31–56.

Price, J., 1981: Upper ocean response to a hurricane. *J. Phys. Oceanogr.,* **11,** 153–175.

Reynolds, R. W., and T. M. Smith, 1994: Improved global sea surface temperature analyses using optimum interpolation. *J. Climate,* **7,** 929–948.

Schmitz, W. J., Jr., 2005: Cyclones and westward propagation in the shedding of anticyclonic rings from the Loop Current. *Circulation in the Gulf of Mexico: Observations and Models, Geophys. Monogr.,* Vol. 161, Amer. Geophys. Union, 241–261.

Shay, L. K., P. G. Black, A. J. Mariano, J. D. Hawkins, and R. L. Elsberry, 1992: Upper-ocean response to Hurricane Gilbert. *J. Geophys. Res.,* **97,** 20 227–20 248.

——, G. J. Goni, and P. G. Black, 2000: Effects of a warm oceanic feature on Hurricane Opal. *Mon. Wea. Rev.,* **128,** 1366–1383.

Teague, W. J., M. J. Carron, and P. J. Hogan, 1990: A comparison between the Generalized Digital Environmental Model and Levitus climatologies. *J. Geophys. Res.,* **95,** 7167–7183.

Yablonsky, R. M., I. Ginis, E. W. Uhlhorn, and A. Falkovich, 2006: Using AXBTs to improve the performance of coupled hurricane–ocean models. Preprints, *27th Conf. on Hurricanes and Tropical Meteorology,* Monterey, CA, Amer. Meteor. Soc., 6C.4. [Available online at http://ams.confex.com/ams/pdfpapers/108634.pdf.]